

Expression studies in gliomas and glial cells do not support a tumor suppressor role for *LGI1*¹

Tiziana Piepoli, Cemile Jakupoglu, Wenli Gu, Elena Lualdi,² Blanca Suarez-Merino, Pietro L. Poliani, Maria Grazia Cattaneo, Barbara Ortino, Dorota Goplen, Jian Wang, Rosa Mola, Francesca Inverardi, Carolina Frassoni, Rolf Bjerkvig, Ortrud Steinlein, Lucia M. Vicentini, Oliver Brüstle, and Gaetano Finocchiaro³

Department of Experimental Research and Diagnostics, Istituto Nazionale Neurologico C. Besta, Milan 20133, Italy (T.P., E.L., B.S.-M., P.L.P., B.O., R.M., F.I., C.F., G.F.); Institut für Rekonstruktive Neurobiologie, University of Bonn, Life and Brain Center and Hertie Foundation, 53105 Bonn, Germany (C.J., O.B.); Institute of Human Genetics, Ludwig Maximilians University Munich, University Hospital, Munich 80336, Germany (W.G., O.S.); Department of Anatomy and Cell Biology, University of Bergen, Bergen N-5009, Norway (D.G., J.W., R.B.); Department of Pharmacology, University of Milan, Milan 20129, Italy (M.G.C., L.M.V.)

Disruptions of *LGI1* in glioblastoma (GBM) cell lines and *LGI1* mutations in families with autosomal dominant epilepsy imply a role for *LGI1* in glial cells as well as in neurons. Although we and others could not find *LGI1* mutations in malignant gliomas, our initial studies appeared to support the idea that *LGI1* is poorly expressed or absent in these tumors. Microarray data suggested that *LGI1* could be involved in the control of matrix metalloproteinases, and we found that tumors derived from U87 glioblastoma cells overexpressing

LGI1 were less aggressive than U87 control tumors. To our surprise, we observed that *LGI1* expression after differentiation of murine neural stem cells was robust in neurons but negligible in glial cells, in agreement with immunohistochemistry studies on rodent brain. This observation could suggest that the variable levels of *LGI1* expression in gliomas reflect the presence of neurons entrapped within the tumor. To test this hypothesis, we investigated *LGI1* expression in parallel with expression of the neuronal marker *NEF3* by real-time PCR on

Received September 17, 2005; accepted October 26, 2005.

¹This work has been supported by a grant to G.F. from Associazione Italiana per la Ricerca sul Cancro (Italian Association for Cancer Research).

Oliver Brüstle holds patent EP 98 966 877.3 relating to embryonic stem cell differentiation into neural precursors.

²The present address of Elena Lualdi is Istituto Nazionale Tumori, Milan, Italy.

³Address correspondence to Gaetano Finocchiaro, Istituto Nazionale Neurologico Besta, via Celoria 11, 20133 Milan, Italy (finocchiaro@istituto-besta.it).

⁴Abbreviations used are as follows: BSA, bovine serum albumin; CP, cortical plate; Cy, indocarbocyanine; DMEM, Dulbecco's modified

Eagle's medium; E, embryonic day; EAR, epilepsy-associated repeat; EGF, epidermal growth factor; eGFP, enhanced green fluorescent protein; ES, embryonic stem; ESNP, embryonic stem cell-derived neural precursor; FACS, fluorescence-activated cell sorting; FGF-2, fibroblast growth factor 2; FITC, fluorescein isothiocyanate; GAPDH, glyceraldehyde 3-phosphate dehydrogenase; GBM, glioblastoma multiforme; GFAP, glial fibrillary acidic protein; *LGI1*, leucine-rich, glioma-inactivated 1 gene; LRR, leucine-rich repeat; *MASS1*, monogenic, audiogenic seizure susceptibility 1 gene; MMP-3, matrix metalloproteinase 3; NEF3, neurofilament 3; OMIM, Online Mendelian Inheritance in Man; PBS, phosphate-buffered saline; PDGF, platelet-derived growth factor; PI3-K, phosphoinositide 3-kinase; RT, real time; TIMP-3, tissue inhibitor of matrix-metalloproteinase 3.

⁵Supplementary figures and tables for this article may be viewed online at http://www.brainlife.org/supplemental/piepoli_t2006.htm.

30 malignant gliomas. Results showed a strong, positive correlation between the expression levels of these two genes ($P < 0.0001$). Thus, our data confirm that *LG11* is involved in cell-matrix interactions but suggest that its expression is not relevant in glial cells, implying that its role as a tumor suppressor in gliomas should be reconsidered. *Neuro-Oncology* 8, 96–108, 2006 (Posted to *Neuro-Oncology [serial online]*, Doc. D05-0007, March 2, 2006. URL www.dukeupress.edu/neuro-oncology; DOI: 10.1215/15228517-2005-006)

Keywords: epilepsy, glioma, invasion, metalloproteinase, migration, tumor suppressor gene

L *GI1*,⁴ the leucine-rich, glioma-inactivated 1 gene, was first identified by studying rearrangements caused by a t(10;19)(q24;q13) balanced translocation in the T98G glioblastoma multiforme (GBM) cell line; rearrangements of the *LG11* gene were also detected in the A172 GBM cell line and in several primary GBMs (Chernova et al., 1998). The *LG11* gene was subsequently found altered, usually by point mutations, in ADPEAF (autosomal dominant partial epilepsy with auditory features [OMIM entry 600512]), a rare form of idiopathic lateral temporal lobe epilepsy characterized by partial seizures with auditory disturbances (Gu et al., 2002; Kalachikov et al., 2002; Morante-Redolat et al., 2002). These observations imply that *LG11* is expressed in glial cells and in neurons and that its altered function can be at least partly responsible for two such different diseases as glioblastoma multiforme and epilepsy. Presently, available data provide only partial hints at an understanding of *LG11* function. *LG11* is part of a gene family, including other *LG11*-like genes. Senechal et al. (2005) have shown that all *LGI* genes encode secreted protein products. *LG11*, in particular, encodes a protein with a calculated molecular mass of 60 kDa that contains 3.5 leucine-rich repeats (LRRs) with conserved flanking sequences. In the LRR domain, *LG11* protein has the highest homology with a number of transmembrane and extracellular proteins that function as receptors and adhesion proteins (Chernova et al., 1998). Sequence analysis of proteins encoded by *LG11* and *MASS1* (monogenic, audiogenic seizure susceptibility 1), a gene mutated in the Frings mouse model of audiogenic epilepsy and in one family with febrile and afebrile seizures (Nakayama et al., 2002; Skradski et al., 2001), identified another homology domain called EAR (epilepsy-associated repeat) consisting of a sevenfold repeated 44-residue motif (Scheel et al., 2002). In the *MASS1* gene product, a fragment of the very large G-protein-coupled receptor 1 (VLGR1), the EAR domain is part of the ligand-binding ectodomain.

Previous data have suggested that there is a loss or reduction of *LG11* expression at the transition from low-grade to high-grade gliomas, and *LG11* was therefore proposed to be a tumor suppressor gene (Kunapuli et al., 2003). Expression of the *LG11* gene product has also been linked to downregulation of a number of matrix metalloproteinases, further suggesting a role for *LG11* in suppressing the invasion phenotype of glioma cells (Kunapuli et al., 2004). However, mutations in the *LG11*

coding region were never found in malignant gliomas, and data following gene transfer in cell culture were conflicting (Krex et al., 2002). To gain further insight on the biologic function of *LG11*, we have studied the expression pattern of the *LG11* gene in differentiating embryonic stem (ES) cells, adult brain, and tumor tissues. Further, we have used the Affymetrix (Santa Clara, Calif.) GeneChip system U95Av2 on U87 cells engineered to express the *LG11* gene product. In vivo experiments with CD1 nude mice showed a slower tumor proliferation in those animals inoculated subcutaneously and intracranially with U87 cells forced to express *LG11* than in those injected with U87 transfected with vector only.

Our data point to a role for *LG11* in the organization of cell-matrix interactions and particularly in the relationships of the tissue inhibitor of matrix metalloproteinase 3 (TIMP-3) with other related factors. Thus, the *LG11* gene product, which is expressed mainly in neural tissues, may contribute to epileptogenesis by affecting neural migration. Its low expression in malignant gliomas appears as a consequence of *LG11* downregulation in glial cells rather than of inactivation by tumor development.

Materials and Methods

LG11 Expression and Sequence Analysis in Primary Tumors and in Cell Lines

Total RNA was isolated from cell lines and tumor samples with Eurozol (EuroClone, Milan, Italy). For real-time (RT)-PCR analysis, 1 μ g of total RNA was first treated with DNase I (Roche, Basel, Switzerland) at 37°C for 40 min and then reverse transcribed with Expand Reverse Transcriptase (Roche) according to manufacturer's instructions. PCR was performed with AmpliTaq Gold (Applied Biosystems, Foster City, Calif.) for 30 cycles by using specific primers on exon 5 and exon 6 (GT3: 5'-cgaactcctttgatgtgatc-3' and GT4: 5'-cttcgcagtagatgtcttca3', respectively). The results were normalized on beta-actin.

For most RT-PCR analysis, we used the TaqMan system (GeneAmp 5700 Detection Systems from Applied Biosystems). Primers and probes for the *LG11* and neurofilament 3 (*NEF3*) genes were obtained from the Assays-on-Demand choice of Applied Biosystems. We used the TaqMan Universal PCR master mix with AmpErase UNG (uracil-N-glycosylase) in a 20- μ l reaction volume following cycling conditions recommended by the manufacturer (Applied Biosystems). Each reaction was carried out in triplicate, together with a negative control (water as template). The *18S* gene was used as an endogenous control (Applied Biosystems). The amplification values obtained from *NEF3* and *LG11* genes were divided by the corresponding amplification values for *18S* to produce an expression index. Statistical comparisons of the two groups were performed by using the Fisher's exact test within the StatView 4.5 software (Abacus Concepts, Inc., Berkeley, Calif.). We ana-

lyzed the coding sequence of *LG11* by direct sequencing of PCR products from tumor genomic DNA. Primer sequences, PCR, and sequencing conditions are available on request.

In Vitro Studies with U87 Cells

U87 cells were originally obtained from ATCC (American Type Culture Collection, Manassas, Va.) and cultured as suggested by the supplier. *LG11* was first cloned in the retroviral vector pLXSN (Clontech, Mountain View, Calif.). Cells were transfected with pLXSN (mock) and pLX-LGI1 by FuGene 6 Transfection Reagent (Roche). Transfected cells were selected by G418. Proliferation studies were done by cell counts (trypan blue) and by colorimetric WST assay (Roche).

Tumor spheroids were initiated as described elsewhere (Goldbrunner et al., 1997; Pilkington et al., 1997). Briefly, both labeled U87-mock and U87-LGI1 suspensions were seeded into culture flasks base coated with 0.75% agar noble in RPMI medium. After five to seven days, 200- μ m spheroids were chosen for coculture assay. Brain cell aggregates were made from brains of fetal BD-IX rats as previously described (Bjerkvig et al., 1986). Briefly, mature brain cell aggregates (300 μ m in diameter) were transferred individually into agar-coated 96-well culture dishes (Nunc, Rochester, N.Y.). Thereafter, similarly sized tumor spheroids were transferred to the wells containing aggregates, and the tumor spheroids were brought into proximity with the aggregates by using a sterile syringe. The cocultures were visualized, after 48 h, by fluorescence microscopy or confocal microscopy (Leica TCS-NT, Heidelberg, Germany).

U87 cell migration and invasion were evaluated by means of chemotaxis and chemoinvasion experiments in a 48-well, modified Boyden chamber (NeuroPore, Gaithersburg, Md.). The chemotaxis experiments were performed by using 8- μ m Nucleopore (Nucleopore, Pleasanton, Calif.) polyvinylpyrrolidone-free pyrocarbonate filters coated with 10 μ g/ml of type IV collagen and placed over a bottom chamber containing 20 ng/ml of platelet-derived growth factor (PDGF) as the chemoattractant factor. U87-LGI1 and U87 mock cells were added to the upper chamber at a density of 3×10^{-4} cells per well. After 6 h of incubation at 37°C, the nonmigrated cells were scraped, and cells that had migrated to the lower side of the filter were stained by Diff-Quick stain (VWR Scientific, Bridgeport, N.J.): Five to eight unit fields per filter were counted at 160 \times magnification by using a Zeiss microscope (Zeiss, Göttingen, Germany). The assays were run in triplicate. For the chemoinvasion assays, the filters were coated with a layer of Matrigel (BD Biosciences, San Jose, Calif.) (100 μ g/filter), a solubilized basement membrane preparation extracted from the Engelbreth-Holm-Swarm mouse sarcoma, which reproduces in vitro the peritumoral matrix that the cells must degrade in vivo to invade the neighboring tissue. The Boyden chamber was assembled with the coated side of the filter facing the cells in the upper compartment. The assays were then performed as described for chemotaxis.

In Vivo Experiments with U87-LGI1 and U87-Mock Cells

Mice were housed in a ventilated cabinet with constant and controlled temperature under a 12-h light schedule. Subcutaneous injections were done on nu/nu female mice (20 g; Charles River Italia, Calco, Italy) with 3×10^{-5} transfected U87 cells (21 U87-mock, 21 U87-LGI1). Tumor growth was measured with a caliper. After 30 days, the animals were sacrificed, and tumors were removed and weighed. Tumors were partially fixed with Carnoy's fixative and were paraffin embedded or partially frozen to isolate RNA.

Intracerebral inoculi, containing 1×10^{-5} transfected U87 cells in 3 μ l of phosphate-buffered saline (PBS), were introduced into nu/nu mice (23 U87-mock and 24 U87-LGI1 in three experiments) placed in a stereotaxic frame. Survival was analyzed by the log-rank (Mantel-Cox) test in Kaplan-Meier nonparametric analysis, using the StatView 4.5 software. Whole brains were fixed in Carnoy's fixative or frozen. Other nude mice were inoculated intracerebrally (i.c.) with 1×10^{-5} cells and sacrificed on day 15 (one U87-mock and two U87-LGI1) and day 21 (two U87-mock and two U87-LGI1) after injection. Adult C57Bl6J mice were sacrificed and processed for in vivo analysis of *LG11* expression. All the mice were terminally anesthetized with CO₂ and transcardially perfused with 50 ml of 0.1% heparin-PBS followed by 4% paraformaldehyde-PBS.

Microarray Analysis

We compared the results obtained from the chips hybridized with U87-mock and U87-LGI1 cRNAs. To obtain cRNAs, total RNA was first isolated from U87-mock and U87-LGI1 cells with the RNeasy kit (Qiagen, Venlo, The Netherlands). The RNA status was controlled on a 1% agarose gel stained with ethidium bromide. First, 15 μ g of total RNA was reverse transcribed to cDNA with Superscript Choice System (Gibco BRL Life Technologies, Gaithersburg, Md.) by using T₇-(dT)₂₄ primer. Double-stranded cDNA was synthesized and then purified by separation with phenol-chloroform-isoamyl alcohol. This cDNA was used for in vitro transcription to cRNA by using the Enzo BioArray kit (Affymetrix). During this step, the cRNA product was labeled with biotin. Following a cleanup with Qiagen RNeasy spin columns, the labeled cRNA was quantified, and 20 μ g was fragmented at 94°C for 35 min. The product was controlled on a 1% agarose gel to verify the distribution of RNA fragments from approximately 35 to 200 bases. The fragmented, biotinylated cRNA was used to hybridize the Human Genome U95A chip (oligonucleotide microarray technology, Affymetrix) following the manufacturer's instructions.

Within each experiment, a dilution series of the transcript and of glyceraldehyde 3-phosphate dehydrogenase (GAPDH) PCR products was processed to demonstrate that amplification efficiencies of target and reference DNA were approximately equal.

Raw data were analyzed by using the MAS5 program

(Affymetrix). Results were validated by RT-PCR by using the SYBR Green kit with GeneAmp 5700 Detection Systems (Applied Biosystems) and primer designed by PrimerExpress (Applied Biosystems). Results were normalized on GAPDH values.

Immunocytochemistry, Histology, and Immunohistochemistry

Anti-LGI1 antibodies were raised in rabbits injected with two human LGI1 peptides conjugated with ovalbumin. Peptide sequences were the following: nh2-FIKIQDIE-ILKIRK-cooh (peptide 716, corresponding to aa 318–331) and nh2-NTQIYKHHVIVDLSA-cooh (peptide 717, corresponding to the last amino acid residues of the C-terminal region). Both peptides were conjugated with ovalbumin and mixed in a 1:1 ratio before injection.

For immunocytochemical analysis, cells were fixed for 20 min with 4% paraformaldehyde in PBS pH 7.4, washed in PBS, permeabilized for 5 min in 0.2% NP-40 in PBS, and then blocked for 45 min with 2% normal human serum and 0.5% bovine serum albumin (BSA) in 0.1% PBS-Triton X-100. Cells were then incubated at 4°C overnight with the primary antibodies (rabbit anti-LGI1 polyclonal, 1:300; and mouse antihuman TIMP-3 monoclonal, 1:5000 [Chemicon, Temecula, Calif.]) in 0.5% BSA-PBS. Cells were washed in PBS and incubated at room temperature for 60 min with indocarbocyanine 3 (Cy3)-conjugated goat antimouse (1:200), Cy3-conjugated goat antirabbit (1:400), fluorescein isothiocyanate (FITC)-conjugated goat antimouse (1:100), or FITC-conjugated goat antirabbit (1:200) secondary antibodies (all from Jackson ImmunoResearch Laboratories, West Grove, Pa.) prepared in 0.5% BSA-PBS. Samples were washed three times in PBS and coverslipped with a mounting medium containing 4',6-diamidino-2-phenylindole (Vector Laboratories, Burlingame, Calif.) to counterstain the nuclei before examination by fluorescence microscopy. Digital images were acquired with a Zeiss Axioskop fluorescence microscope. For bright-field staining after the primary antibody incubation, cells were incubated at room temperature for 60 min with biotin-labeled secondary goat antirabbit (1:200 [Dako, Glostrup, Denmark]) or goat antimouse (1:100 [Dako]) antibodies, and the signal was detected with streptavidin-conjugated horseradish peroxidase (1:300, Dako) and diaminobenzidine.

Experiments on rat embryos (Sprague-Dawley, Charles River, Calco, Italy) were performed on embryonic day (E) 15 and E19. The day of detection of a vaginal plug was designated as E1. All the experiments were undertaken in accordance with the guidelines established in the European Union principles of laboratory animal care (Council of European Communities, directive 86/609/EEC). The embryos were obtained from pregnant rats anesthetized with chloral hydrate (4%; 1 ml/100 g of body weight; i.p.) perfused with mixed aldehydes (for details, see Ortino et al. [2003]). The forebrain was dissected out and coronally cut with a Vibratome (St. Louis, Mo.) in 50- to 60- μ m-thick serial sections or paraffin embedded and cut into 7- μ m-thick sections

on gelatin-coated slides. For single immunolabeling, paraffin-embedded sections were incubated overnight with polyclonal antibody LGI1 (1:300). The avidin-biotin-peroxidase complex protocol (ABC method, Vector) was used for the immunohistochemical procedure with 3,3'-diaminobenzidine as chromogen. Immunoreacted sections were then counterstained with thionine for identification of the developing region of the telencephalon. For double-immunofluorescence experiments, free-floating sections were incubated in a cocktail (mixture) of the LGI1/TuJ11 (BAbCO, Richmond, Calif.) (1:300/1:8000) or LGI1/VIM (Dako) (1:300/1:200) and subsequently in a mixture of the corresponding secondary antibodies (Jackson ImmunoResearch Laboratories), Cy2-conjugated horse antimouse (1:200) and Cy3-conjugated goat antirabbit (1:600). After repeated rinsing, sections were mounted in Fluorsave (Calbiochem, San Diego, Calif.) and examined in a confocal laser scanning microscope (Bio-Rad, Hemel Hempstead, UK) equipped with an argon-krypton mixed-gas laser with excitation peaks at 510 nm (for Cy2) and 550 nm (for Cy3). Confocal image series were recorded through separate channels to avoid cross talk and merged with Bio-Rad LaserSharp 2000 software.

For experiments on mouse brain, paraffin-embedded brains were cut at 4- μ m thickness on a microtome and stained for histological examination. Tumor size and distribution were evaluated on routine hematoxylin and eosin-stained slides. The expression of LGI1 throughout the brain was assayed by immunohistochemistry by using the same antibodies and dilutions described previously.

Cultivation of Embryonic Stem Cell-Derived Neural Precursors

Mouse J1 ES cells were differentiated in vitro into neuronal and glial committed precursor cells according to previously described protocols (Brustle et al., 1999; Okabe et al., 1996). Briefly, proliferating mouse ES cells (stage 1) were expanded on irradiated mouse embryonic fibroblasts in Dulbecco's modified Eagle's medium (DMEM) (Invitrogen, Karlsruhe, Germany) supplemented with 20% fetal bovine serum (AG Seromed, Biochrom, Berlin, Germany), 1 \times MEM-essential amino acids (Invitrogen), 8 mg/liter adenosine, 8.5 mg/liter guanosine, 7.3 mg/liter cytidine, 7.3 mg/liter uridine, 2.4 mg/liter thymidine, 0.1 mM 2-mercaptoethanol, 26 mM HEPES (all from Sigma, Taufkirchen, Germany), and 103 U/ml leukemia inhibitory factor (Chemicon, Hofheim, Germany). After passaging onto gelatin-coated dishes (0.1% gelatin; Sigma), ES cells were trypsinized and transferred to bacterial dishes to allow embryoid body formation. Embryoid bodies were propagated for four days in the absence of leukemia inhibitory factor and subsequently plated onto tissue culture dishes. One day after plating, the medium was replaced by ITSFn (insulin, transferrin, selenium, and fibronectin) (stage 2) (i.e., DMEM/F12, Invitrogen) supplemented with 5 g/ml insulin, 50 g/ml human apotransferrin (both from InterGene, Purchase, N.Y.), 30 nM sodium selenite (Sigma,

St. Louis, Mo.), 2.5 g/ml fibronectin (Life Technologies, Karlsruhe, Germany), and penicillin-streptomycin (Invitrogen). This medium has been shown to favor the survival of neuroepithelial cells (Okabe et al., 1996). After five days, cells were triturated to a single-cell suspension and further propagated on polyornithine-coated dishes (15 µg/ml, Sigma) in the presence of 10 ng/ml fibroblast growth factor 2 (FGF-2). This permits the proliferation of pan-neural precursors, which can be differentiated by growth factor withdrawal into neuronal as well as glial cells. The proliferating pan-neural precursor cells were either growth factor withdrawn for four days (stage 3) and eight days (stage 4) or further proliferated in different media for glial cell enrichment. To obtain proliferating glial precursors, ES cells were again dissociated and proliferated in the presence of 10 ng/ml FGF-2 and 20 ng/ml epidermal growth factor (EGF) (stage 5). After four days of growth factor withdrawal, these cells were driven into a mixed population of astroglial and oligodendroglial cells (stage 6). Proliferating cells from stage 5 were further grown in a medium containing 10 ng/ml FGF-2 and 10 ng/ml PDGF (stage 7), which has been shown to enhance oligodendroglial differentiation upon growth factor withdrawal (Glaser et al., 2005). Cells from stage 7 were differentiated by four days of growth factor withdrawal (stage 8). All growth factors (FGF-2, EGF, and PDGF) were purchased from R&D Systems (Wiesbaden, Germany).

Quantitative RT-PCR of ES Cell-Derived Neural Precursors

Embryonic stem cell-derived neural precursors (ESNPs) from proliferating and differentiated pan-neural (stages 3 and 4) and glial (stages 5–8) precursor stages were used for Trizol (Invitrogen) extraction of RNA. Total RNA from cultured cells was phenol extracted with TriFast (Peqlab, Erlangen, Germany) and treated with RNase-free DNase (Promega, Madison, Wis.). From each sample, 1 µg of total RNA was transcribed into cDNA by using an iScript cDNA synthesis kit (Bio-Rad, Munich, Germany) according to the manufacturer's instructions. All qRT-PCR experiments were performed in triplicate on an i-cycler (Bio-Rad) with *GAPDH* as the reference gene for normalization and SYBR I Green for fluorescence detection. To test whether the expression of *GAPDH* remains constant in the analyzed samples, we quantified the expression levels of 18S RNA. The differences in expression of these two genes remained similar in all of the cell populations examined. Threshold cycle (C_T) was measured as the cycle number at which the SYBR Green emission increases above the threshold line. Specific mRNA transcript levels were calculated by using Q-Gen Core Module 1.2 software (Muller et al., 2002). PCR product specificity was controlled by melt curve analysis and visualized by agarose gel electrophoresis. All used primers, with the exception of *GAPDH*, all were intron spanning, and sequences were as follows: *GAPDH* forward 5'-acgacccttcattgacctcaact-3' and reverse 5'-atatttctctggtggtcacacct-3'; *LG11* forward 5'-atcttctggaatgggaccacgtag-3' and reverse 5'-tgaggtgtct-

gaggccaatggt-3'; glial fibrillary acidic protein (*GFAP*) forward 5'-gagttaccagatctactcaac-3' and reverse 5'-ccaagctctttaccacgatg-3'; and *Tubb3* forward 5'-gatgatgacgaggaatcgaa-3' and reverse 5'-cagatgctgctgtcttggc-3'.

Acute Cell Isolation and Fluorescence-Activated Cell Sorting of Juvenile Brain

Glial fibrillary acidic protein-enhanced green fluorescent protein (GFAP-eGFP) transgenic mice (Nolte et al., 2001) at the age of 8 and 14 days were sacrificed. The brain regions were cut into 1-mm³ pieces and papain digested for 40 min before single-cell trituration. Media for cell dissociation were used as described for cell dissociation of embryonic cortical neurons (Polleux and Ghosh, 2002). The cell suspensions were kept on ice and were purified by fluorescence-activated cell sorting (FACS) of GFAP-eGFP-positive cells by using a FACSDiVa cell sorter (BD Biosciences). After sorting, the GFP-positive and GFAP-negative cells were FACS analyzed for sorting efficiency and immediately frozen for RNA purification.

Results

LG11 Expression Is Often Low in Malignant Gliomas

We analyzed *LG11* expression by semiquantitative PCR in a panel of eight different normal tissues, in 70 gliomas (5 grade I, 19 low-grade glioma, 11 grade III, and 35 GBMs) and in six cell lines (human malignant gliomas U373, U138, SW 1088, U87, and U118 and murine malignant glioma GL261). In 16 (45.7%) of 35 GBMs, *LG11* expression was very low or absent and was completely absent in all cell lines. In only two of 35 low-grade gliomas, *LG11* expression was decreased or absent, while in other cases, expression levels were comparable to normal brain (two samples examined), confirming previous data (Besleaga et al., 2003; Chernova et al., 1998). (See supplementary data, Fig. 1S.⁵)

To look for mutations of *LG11*, the complete coding sequence was analyzed in 10 GBMs after PCR amplification with intronic primers. No mutations were found, which was in agreement with previous observations (Krex et al., 2002; Somerville et al., 2000).

Expression of *LG11* Decreases Tumorigenicity of U87 GBM Cells

The effect of *LG11* on cell proliferation was studied on the human GBM cell line U87, which does not express *LG11*, as shown by RT-PCR (Fig. 1A). *LG11* was first inserted into the retroviral plasmid pLXSN, creating pLX-*LG11*, and then U87 cells were transfected with pLX-*LG11* or pLXSN as a control and selected by G418. When checked around passage 5, U87-*LG11* cells showed strong *LG11* expression (Fig. 1A).

The clonal analysis performed two days after transfection showed that U87-*LG11* clones formed after 15 days are 16% to 34% of the number formed by U87-

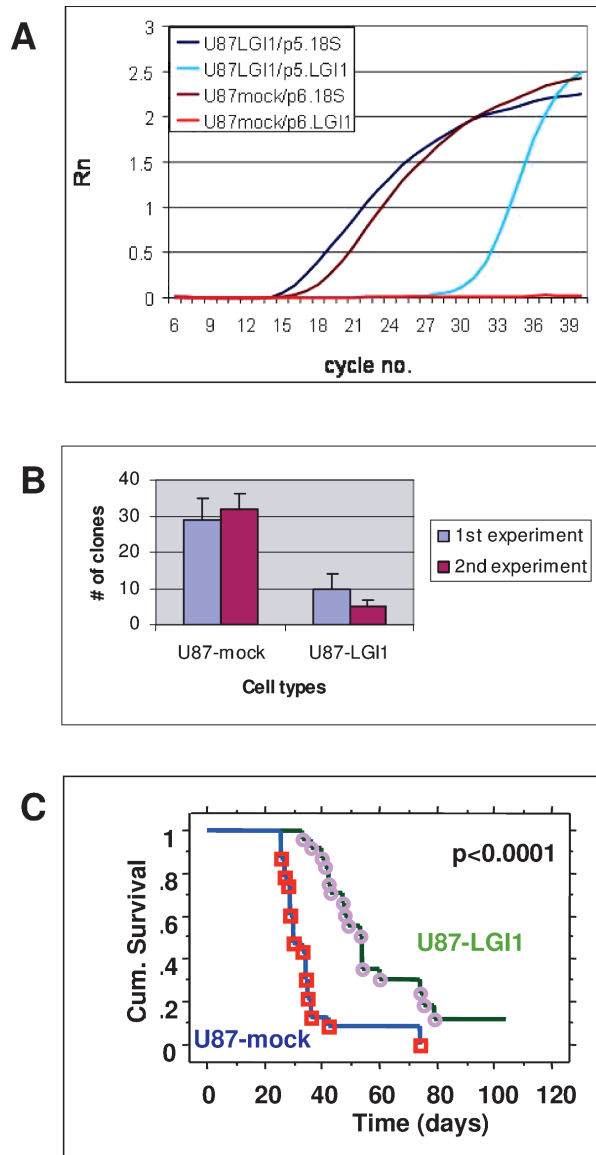


Fig. 1. In vitro and in vivo effects of LGI1 overexpression in U87 cells. A. Real-time PCR profiles of LGI1 and control (18S) amplification of early-passage U87-LGI1 and U87-mock cells. Level of fluorescence (Rn) detected during PCR was determined by dividing the probe reporter dye signal by the passive reference signal. B. Cloning potential of U87-mock and U87-LGI1 cells after limiting dilution. C. Survival of CD1 nude mice after intracranial injection of U87-LGI1 and U87-mock cells. The Kaplan-Meier analysis combines results of three independent experiments.

mock cells (Fig. 1B). Analysis by the WST1 proliferation assay on cells that had been passaged more than five times (i.e., at least two months after transfection) did not show any significant difference in the proliferation rate (data not shown).

To look for in vivo tumorigenicity of U87-LGI1 and U87-mock cells, we inoculated female CD1 nude mice subcutaneously with 3×10^5 cells of the two types ($n = 21$ for each group). After 30 days, the weight of U87-LGI1 tumors was 45% that of U87-mock tumors (28.8 ± 39.8 vs. 63.8 ± 68.6 mg; $P = 0.0499$). *LGI1* expres-

sion measured by RT-PCR in four U87-LGI1 tumors was $24.2\% \pm 17.2\%$ that in U87-LGI1 cells, which suggests that in vivo *LGI1* expression was selected against (data not shown). We then performed three experiments inoculating 3×10^5 U87-LGI1 or U87-mock cells into the brain of nude mice ($n = 47$ overall; see Materials and Methods): Animals inoculated with U87-LGI1 cells survived significantly longer than controls inoculated with U87-mock cells ($P < 0.0001$; Fig. 1C).

DNA Microarray Analysis Demonstrates Upregulation of TIMP-3 Expression in U87-LGI1 Cells

To gain insight on *LGI1* function, we performed two independent experiments comparing expression profiles of U87-LGI1 and U87-mock cells using the human gene chip U95 from Affymetrix. With this approach, we identified 18 probe sets downregulated and 23 probe sets upregulated in *LGI1*-transfected U87 cells as compared to those in mock-transfected cells (see supplementary data, Table 1S⁵). We then focused on transcripts that could be linked to the role played by *LGI1* in GBM containment: One of these 41 genes, *TIMP-3*, appeared as a good candidate, since it is an important negative regulator of tumor invasion, promotes tumor apoptosis (Baker et al., 1999), and is often silenced in different malignancies, including gliomas (Bachman et al., 1999).

Using RT-PCR on cDNAs from U87-mock and U87-LGI1 cells used in microarray experiments and on cDNAs obtained independently from the same cells, we confirmed that *TIMP-3* is upregulated when *LGI1* is expressed (Fig. 2). We then looked for other genes whose expression could potentially be influenced by *TIMP-3*. Matrix metalloproteinase 3 (MMP-3, or stromelysin 1) was a first, obvious candidate because this matrix metalloproteinase is controlled by *TIMP-3* (Apte et al., 1995) and is active in gliomas (Arato-Ohshima and Sawa, 1999; Nakano et al., 1993). In both experiments, the expression of MMP-3 (accession no. X05232) was lower in U87-LGI1 cells than in U87-mock cells. We then investigated by RT-PCR the MMP-3 expression in U87-LGI1 and U87-mock cells and found that indeed *LGI1* expression was associated with a fivefold decrease in MMP-3 expression (Fig. 2). The ELISA analysis performed on the supernatant of U87-mock and U87-LGI1 cells showed higher levels of MMP-3 in the supernatant of U87-mock cells (68 ng/ml) than in that of U87-LGI1 cells (34 ng/ml; see supplementary material, Fig. 2S⁵).

We then studied by immunocytochemistry *LGI1* and *TIMP3* expression in U87-mock and U87-LGI1 cells. The *LGI1* antiserum that we obtained by immunization against *LGI1* peptides could effectively stain early-passage U87-LGI1 cells but not U87-mock cells. The same pattern was obtained by staining with commercially available anti-*TIMP3* antibodies (see supplementary material, Fig. 3S⁵). Immunohistochemistry was also performed 15 days after injection of U87-LGI1 and U87-mock cells into the brain of CD1 nude mice. U87-LGI1 tumors, stained by anti-*LGI1* antibodies, were smaller than U87-mock tumors and showed higher *TIMP-3* expression (data not shown).

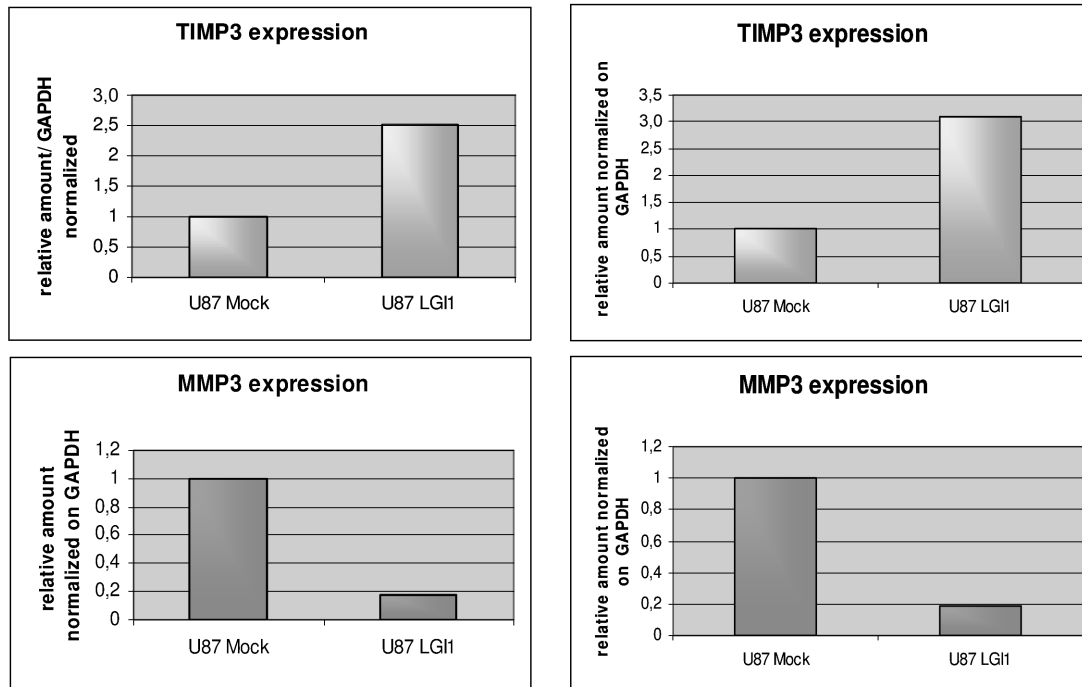


Fig. 2. LGI1 expression is involved in the control of TIMP-3 and MMP-3 expression. The four panels show results of RT-PCR on two independent cDNA samples showing increased expression of TIMP-3 and decreased expression of MMP-3 in U87-LGI1 cells.

LGI1 Is Involved in Cell-Matrix Interactions in the CNS

To validate the role of *LGI1* in the regulation of invasion processes, we set up an in vitro experiment to test interactions of U87-mock and U87-LGI1 spheroids with fetal brain aggregates. After 48 h, U87-mock cells showed an extensive invasion into the brain cell aggregates (Fig. 3A). In contrast, the U87-LGI1 cells showed a reduced invasion with a clear-cut demarcation with respect to normal brain tissue (Fig. 3B), confirming the role of *LGI1* in controlling invasion-migration processes.

To quantify cellular invasive activity, we performed Matrigel chemoinvasion experiments in Boyden chambers (Albini et al., 2004). In this assay, we compared the invasive properties of U87-mock and U87-LGI1 cells both in the absence and in the presence of PDGF (20 ng/ml), a growth factor able to induce motility in various cell types, including gliomas (Heldin et al., 1998). As shown in Fig. 3C, the two cell lines retained their ability to invade Matrigel, both under basal conditions and after stimulation with PDGF. The expression of *LGI1* significantly reduced this response, with an inhibition of 50% under basal conditions and 36% in PDGF-stimulated cells ($P < 0.01$).

Phosphoinositide 3-kinases (PI3-Ks) play a crucial role in many different physiological events, including cell migration (Cantley, 2002). AKT is a protein kinase recruited to the membrane and activated by phosphorylation as a consequence of PI3-K activity. Phosphorylated AKT is therefore taken as an index of the activity of class I PI3-Ks. We found that PDGF-induced AKT phosphorylation in U87-LGI1 cells was strongly reduced

in comparison with the response detected in U87-mock cells (see supplementary material, Fig. 4S-A⁵). On the contrary, ERK (extracellular signal-related kinase) activation by PDGF was similar in the two cell lines, indicating that the impairment of the PI3-K pathway in transfected cells is not due to a general stress of the cells, but it is selective for this pathway. That the PI3-K signaling pathway plays a pivotal role in controlling glioma cell movement is strongly indicated by the experiments showing that the PI3-K inhibitor LY294002 reduces by 80% the PDGF-stimulated migration of U87-mock cells and blocks it in U87-MG/LGI1 cells (see supplementary material, Fig. 4S-A and B⁵).

LGI1 Is Predominantly Expressed in Neurons Rather than Glial Cells

Following published protocols (Brustle et al., 1999; Okabe et al., 1996), mouse ES cells were differentiated in vitro into pan-neural (i.e., with potential to differentiate into neuronal as well as glial cells) and subsequently glial cells (for details, see Materials and Methods). FGF-2 withdrawal from pan-neural precursors for four days (stage 3) and eight days (stage 4) induces neuronal differentiation, achieving approximately 60% neurons (Okabe et al., 1996). In the subsequent stages (stages 5–8), the neural precursors drift predominantly into a glial cell fate. Proliferation under EGF/FGF-2 influence (stage 5) induces an astroglial fate upon growth factor withdrawal (stage 6), whereas proliferation under PDGF/FGF-2 administration (stage 7) induces an oligodendroglial fate upon growth factor withdrawal (stage 8) (Glaser et al., 2005).

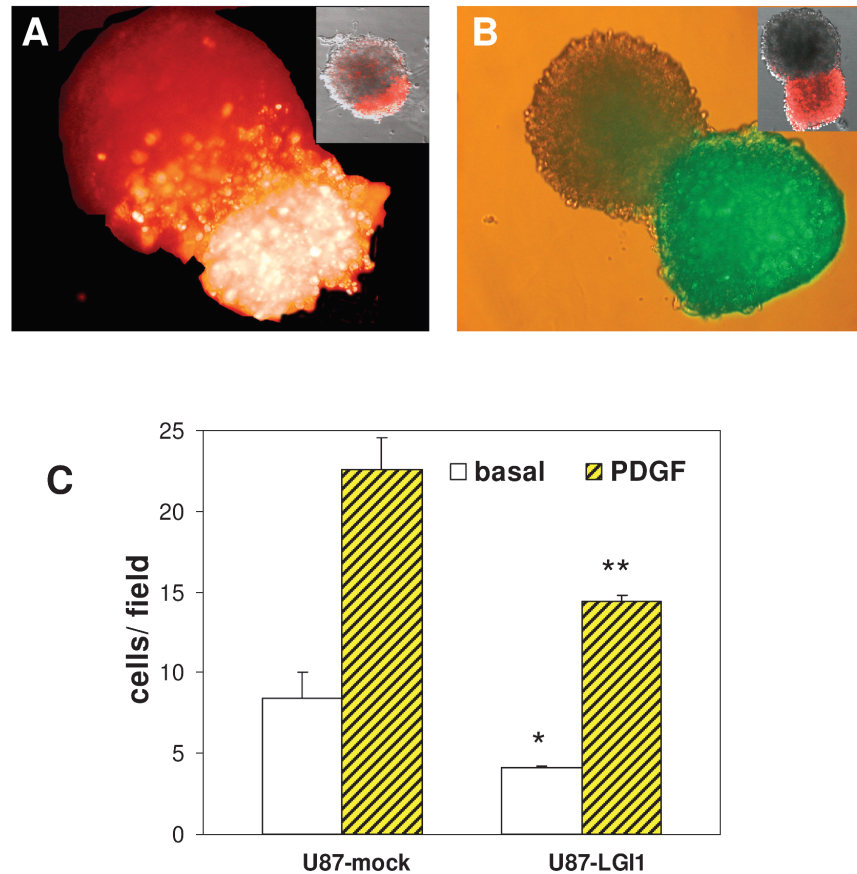


Fig. 3. LGI1 expression is associated with decreased migration of U87 cells. A. A 48-h coculture of U87-mock cells stained with DiI and a fetal brain cell aggregate. An extensive invasion of the normal brain tissue is seen. B. A 48-h coculture of U87-LGI1 cells stained with DiO. A well-defined border is seen between the normal brain tissue and the tumor cells (200 \times). Inserts in panels A and B: Confocal sections 80 μ m inside the cocultures indicating solid infiltration of U87-mock cells (both panel insets: DiI staining, 150 \times). C. U87-mock migration and U87-LGI1 migration were evaluated in the absence (open bar) or in the presence (diagonal bar) of PDGF (20 ng/ml) as an attractant factor. The results are expressed as number of migrated cells and are the mean values \pm SD of a representative experiment, which was performed six times with similar results. * $P < 0.01$; ** $P < 0.001$ compared to U87-mock cells.

To confirm the expected differentiation of the mouse ES cells into neuronal and subsequently glial cells, the neuronal marker Tubb3 and the astroglial marker GFAP were quantified by RT-PCR. Tubb3 was found at least 4-fold to 8-fold higher in stages 3 and 4 than in proliferating or differentiated glial stages (Fig. 4). GFAP was found 14-fold to 120-fold higher in proliferating/differentiated glial stages than in stages 3 and 4 (Fig. 4). *LGII* was at least 18-fold higher expressed in stages 3 and 4 as compared to levels in the subsequent glial stages (Fig. 4), which supports the idea that *LGII* is predominantly expressed in neuronal cells.

GFAP-GFP transgenic mice expressing GFP under the human GFAP promoter (Nolte et al., 2001) were used for acute isolation and flow cytometric separation of GFP-positive and GFP-negative cells from P8 and P14 brain tissues. The sorting efficiencies are shown in Fig. 5A. We compared sort-purified GFP-positive and GFP-negative cells of neocortical, striathalamic, and hindbrain regions. Fivefold increased GFAP levels in the

GFP-positive cells confirmed sort purification. The GFP-negative-sorted cell fraction revealed at least twofold increased levels of Tubb3, indicating an enrichment of neuronal cells (Fig. 5C). *LGII* was found at the highest levels in the GFP-negative cell fractions of cortex and striatum (Fig. 5B), again indicating a preferentially neuronal expression of *LGII*. Regarding the analyzed ages of 8 and 14 days, we found that *LGII* expression was significantly higher in older mice. In summary, we conclude that *LGII* expression is highest in neuronal cells and seems to be upregulated during development.

Double-labeling experiments in E15 embryos, using antibodies against LGI1 and Tuj1 (Tubb3), a marker of migrating and differentiating postmitotic neurons (Lee et al., 1990), revealed that *LGII* was intensely expressed by the migratory cells of the cortical plate (CP) (Fig. 6A). Vimentin-positive, radially oriented glial fibers, which at this developmental stage cross the whole cortex, were interposed within *LGII*-expressing cells in the CP (Fig. 6B), which suggests that some of these young neurons

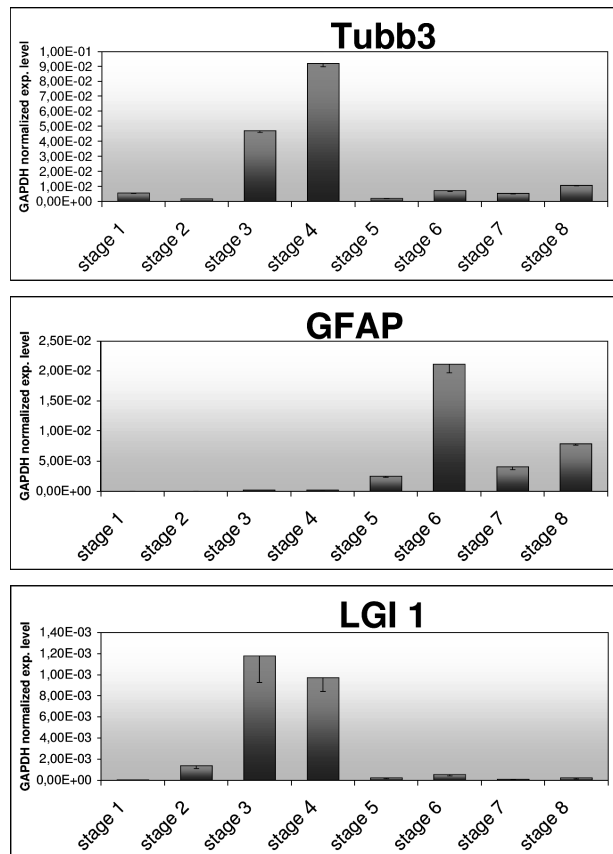


Fig. 4. *LG11* expression during neural cell differentiation. Murine embryonic stem cells (stage 1) were differentiated subsequently into pan-neural stages (stages 3 and 4) and glial stages (stages 5–8) (for details, see Materials and Methods). The highest *LG11* expression was found in stages with high content of neuronal cells, as indicated by high *Tubb3* levels, whereas it was significantly downregulated in later, predominantly glial stages with high *GFAP* content.

reach their final position in the CP by using radial glial fibers. Immune labeling for *LG11* was found at the end of the embryonic development, when the CP is expanding and layer VI is clearly identifiable. Intense immunohistochemical staining was present at E19 in the CP as well as in neurons of layer VI (Fig. 6C and D). In addition, some neuroepithelial precursor cells localized in the ventricular zone were *LG11* positive (Fig. 6E).

We also looked for the expression patterns and the anatomical distribution of *LG11* in adult mouse CNS. *LG11* was highly expressed in neurons of different CNS regions and particularly in cortical, cerebella, hippocampal, and spinal cord neurons (Fig. 6F–I).

In GBM, LG11 Expression Correlates with Expression of the Neuronal Marker NEF3

Since neurons express *LG11* at a high level, we decided to test whether *LG11* expression in gliomas was consequent to the presence of neurons entrapped into the tumor.

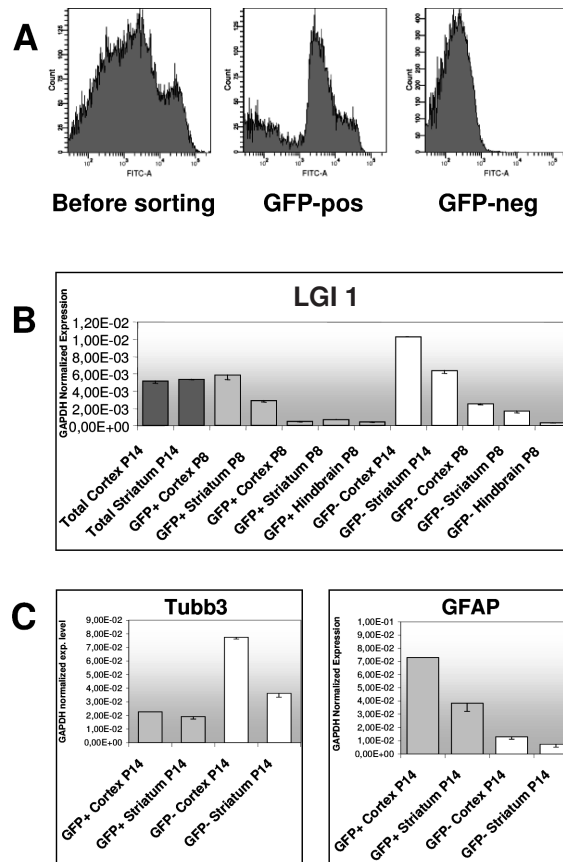


Fig. 5. Patterns of *LG11* expression in postnatal mouse brain. A. P8 and P14 *GFAP*-GFP transgenic mice were used for acute isolation and separation of GFP-positive and GFP-negative cells. Flow cytometric analysis (FITC channel) shows GFP distribution in unsorted, GFP-positively sorted, and GFP-negatively sorted cells. B. *LG11* expression levels were highest in the GFP-negative cortical and striatal cell fractions of P14 and P8 mice. These levels were at least twofold increased as compared to the corresponding GFP-positively sorted glial cells. C. Comparison of the *Tubb3* (neuronal) and *GFAP* (glial) expression in GFP-positive and GFP-negative cell fractions.

To study this, we explored by RT-PCR the expression pattern of the neuronal cell marker *NEF3* and of *LG11* in 30 malignant gliomas (28 GBMs and two anaplastic astrocytomas). Reactions were normalized according to *18S* expression, and expression values were compared to those of commercially available normal brain (Ambion, Austin, Tex.). Simple regression analysis indicated that a significant correlation was present in the expression of these two genes ($r = 0.68$, $P < 0.0001$; Fig. 7).

We also evaluated results considering as low or high the values that were, respectively, below or above the median of the delta cycle threshold (see supplementary data, Table 2S⁵). Again the data indicated a strong correlation between *LG11* expression and *NEF3* expression in GBM by Fisher's exact test ($P = 0.0001$).

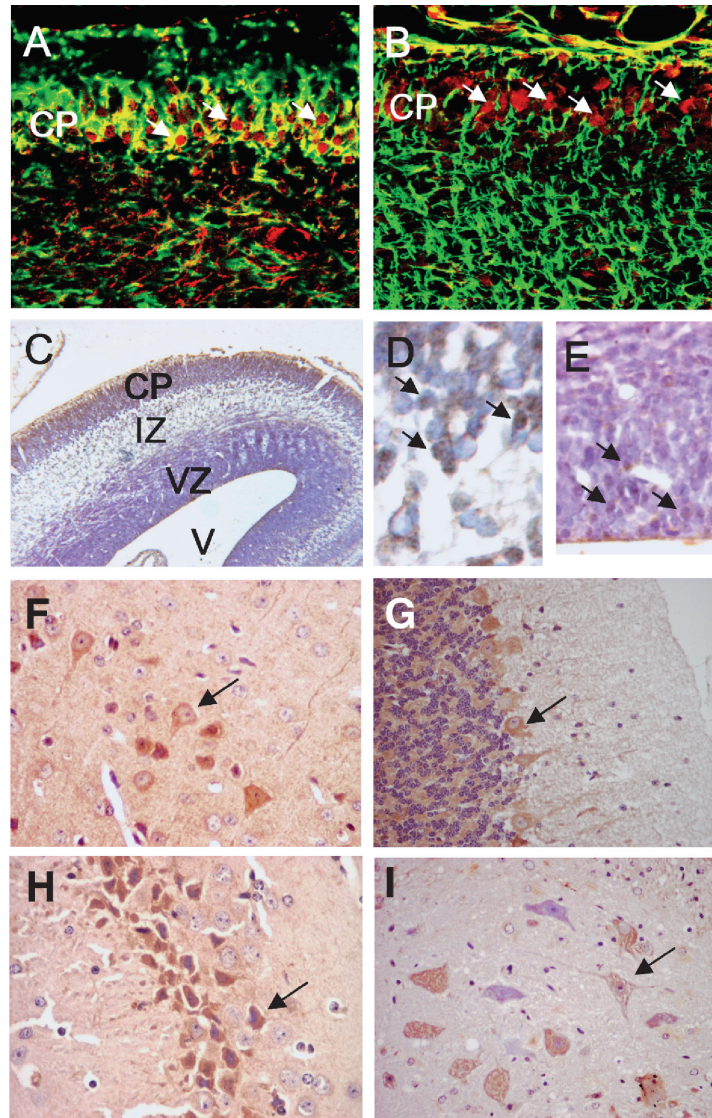


Fig. 6. LGI1 expression during brain development and in adult CNS. A. In double-immunofluorescence experiments performed in coronal sections of E15 rat neocortex examined with confocal laser scanner microscopy, postmitotic neurons in the cortical plate express TuJ1 (green) and LGI1 (red) during the migration phase. Overlap in expression of antigens is shown in yellow (84 \times). B. LGI1-immunoreactive neurons (red, arrows) are interposed within vimentin-positive radial glial fibers (80 \times). C–E. Immunohistochemistry for LGI1 on E19 neocortex coronal sections, counterstained with thionin, shows that LGI1 is expressed predominantly in developing cortical plate, but also in the ventricular zones (6.3 \times). Higher magnification in panel D (80 \times) includes the lower part of cortical plate and the upper part of layer VI, showing intense neuronal immunoreactivity for LGI1. Panel E shows the region of the ventricular zone where some LGI1-immunoreactive cells populate the neuroepithelium (40 \times). (CP, cortical plate; IZ, intermediate zone; VZ, ventricular zone; V, third ventricle). F–I. A strong neuronal staining of LGI1 antibodies is visible in the cortex (panel F, 40 \times), cerebellum (panel G, 40 \times), hippocampus (panel H, 40 \times), and anterior horns of the spinal cord (panel I, 60 \times) of adult murine CNS.

Discussion

Two reports first established that mutations of *LGII* are associated with a dominantly inherited form of epilepsy (Kalachikov et al., 2002; Morante-Redolat et al., 2002). After these findings were published, a number of studies confirmed that *LGII* mutations do play a role in inherited epilepsy (Brodtkorb et al., 2005; Fertig et al., 2003; Gu et al., 2002; Hedera et al., 2004; Michelucci et al., 2003; Pizzuti et al., 2003). On the other hand, the initial

suggestion that *LGII* alterations are implied in glioma tumorigenesis did not receive any direct confirmation. On the contrary, a few reports have cast doubts on such a role (Brodtkorb et al., 2003; Gu et al., 2005; Krex et al., 2001, 2002). In recent years, we have compiled the data presented in this article that, while confirmatory of a role of *LGII* in cell-matrix interactions and migratory processes in the CNS, seem to restrict this role to neuronal and not to glial cells.

Our data do confirm that in malignant gliomas *LGII*

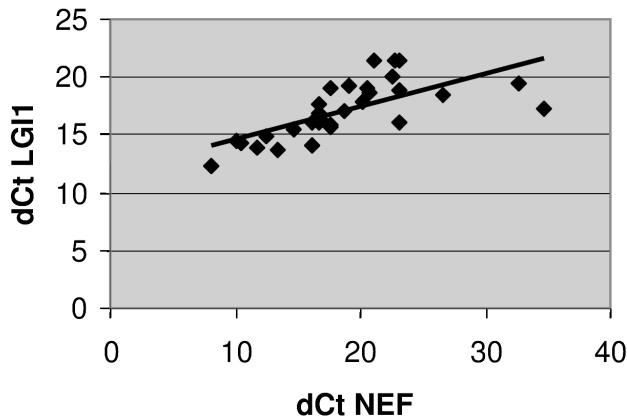


Fig. 7. Correlation between *LG11* expression and *NEF3* expression in malignant gliomas. The graph shows results of the regression analysis on 28 GBMs and two anaplastic astrocytomas. Real-time PCR was performed to assess expression of *LG11* and the neuronal marker *NEF3*. $r = 0.68$; $P < 0.0001$.

expression is often low and, interestingly enough, that it is completely absent in all the glioma cell lines that we have tested. These include U87 GBM cells, one of the cell lines most frequently used in experimental neuro-oncology. Using RT-PCR, we confirmed the absence of *LG11* expression in two U87 lines used in two independent laboratories collaborating in this study (Istituto Nazionale Neurologico C. Besta [G.F.] and University of Hong Kong [S.Y. Leung]). Because of these results and considering the *in vivo* tumorigenicity of U87 cells, we decided to base a relevant part of our work on the study of *LG11* overexpression in this cell line. Kunapuli et al. (2003), however, found that U87 cells express low levels of *LG11* and suggested that this endogenous expression was an obstacle to displaying the results of *LG11* transfection. Interestingly enough, Carson and Pirruccello (1998), using dilutional cloning, obtained five distinct sublines from the parent U87 population; thus, cell culture heterogeneity may explain differences in *LG11* expression found by us and by Kunapuli et al. We have found that in early-passage U87-*LG11* cells the forced expression of *LG11* reduces the clonogenic potential of U87 cells and their migration potential in Matrigel (see Figs. 1B and 3C, respectively). This is in agreement with the data obtained by Kunapuli et al. on A172 and T98 glioblastoma cells overexpressing *LG11*. When we repeated experiments in U87-*LG11* cells passaged more than five times, the effects on both proliferation and migration progressively disappeared. This was in close association with decreased *LG11* expression taking place during culturing in spite of G418 selection, as evaluated by RT-PCR. U87 cells can escape the action of exogenous genes negatively regulating the cell cycle (Tenan et al., 1995). Thus, it is possible that Kunapuli et al. (2003) could not confirm in U87 cells the observations made by *LG11* overexpression on A172 and T98 cells because U87 cells can silence the exogenous expression of *LG11* more effectively than can the other cell lines. This could also explain the difficulties experienced

by Krex et al. (2002) in suppressing S-phase transition by *LG11* overexpression.

Our *in vivo* observations obtained by injecting U87-*LG11* and U87-mock cells in nude mice *s.c.* or into the brain agree with the *in vitro* data, showing for the first time that *LG11* expression can decrease aggressiveness of U87 tumors (Fig. 1C). Microarray data suggested that this function is mediated by inhibition of MMP-3 and by increased expression of TIMP-3. The data were also validated by PCR, ELISA, and immunocytochemistry on U87-*LG11* and U87-mock cells and by *in vitro* experiments on brain spheroids and agree with similar observations performed by Kunapuli et al. (2004).

At the time of these investigations, then, we obtained a set of data coherent with the attribution of a tumor suppressor role to *LG11*. Discrepancies, however, were present. We and others could not find point mutations or microdeletions supporting the relevance of *LG11* as a suppressor (this article; Krex et al., 2002; Somerville et al., 2000). According to the Knudson model, two hits are inactivating tumor suppressor genes: The first one is usually a chromosomal deletion including one gene copy, detectable as a loss of heterozygosity (a frequent finding in the 10q24 region, where *LG11* is located); the second can be a mutation or a chromosomal translocation, as initially reported for *LG11* (Chernova et al., 1998). A further report, however, could not confirm translocations as a general mechanism of *LG11* inactivation (Krex et al., 2002). As exemplified by studies on *CDKN2A*, promoter methylation may be an important mechanism for gene inactivation (Merlo et al., 1995). Analysis on the *LG11* promoter, however, did not show significant differences in the methylation status of normal brain and that of glioblastomas (Somerville et al., 2000).

Another important question on the *LG11* role in gliomas was raised by histological studies on adult mouse brain, showing that *LG11* expression is confined to neurons (Kalachikov et al., 2002; Morante-Redolat et al., 2002), as also confirmed by our observations (Fig. 6F–I). In acutely isolated cells from the juvenile mouse brain, *LG11* expression was highest in neuronal cell fractions of neocortex and striatum. During neural differentiation of murine embryonic stem cells, the *LG11* expression profile strongly corresponded with the profile of the neuronal marker *Tubb3*, whereas *LG11* levels were clearly downregulated in predominantly glial cell stages.

Thus, three different lines of evidence support the idea that *LG11* is not expressed primarily in glial cells, implying that its lack in malignant gliomas is not the consequence of genetic alterations but rather of expression patterns normally occurring during brain development. The results obtained by RT-PCR of *LG11* and *NEF3* expression on 30 malignant gliomas explain the apparent discrepancy in the different expression levels of different gliomas *in vivo*, indicating that such difference is consequent to neuronal cell “contamination” in the tumor specimen.

If this is the case, should we consider as contradictory the data attributing to *LG11* a function in controlling cell-matrix interactions and, therefore, migration/invasion processes? Our results, as well as those of Kunapuli et

al. (2003, 2004), may very well allude to the actual function of *LG11*, but to such function as it physiologically occurs in neurons and not in glial cells. In this regard, it is quite intriguing that *LG11* bears considerable sequence similarity with *SLIT1*, an important repulsive guidance cue for neurons (Cloutier et al., 2004; Yuan et al., 1999) in close collaboration with the slit receptor Rig-1/Robo3 (Marillat et al., 2004).

Although direct evidence linking mutations of guidance genes to epilepsy is not available, recent data provide important suggestions that this may well be the case (Ponnio and Conneely, 2004; Yang et al., 2005). A knockout mouse for *LG11* could provide a relevant tool for these investigations. Unfortunately, our attempts in this direction, performed by deletions of the first exon of *LG11*, have been repeatedly unsuccessful, suggesting that the *LGI1* locus maybe resistant to homologous recombination.

Acknowledgments

We thank Suet Y. Leung (Departments of Pathology and Surgery, University of Hong Kong, Hong Kong, China) for contributing data on *LG11* expression in gliomas; Christiane Nolte and Helmut Kettenmann for providing the hGFAP-eGFP transgenic mouse strain; Cristina Longinotti, Patrizia Tunici, Ettore Salsano, Laura Cajola, Stefania Mazzoleni (all at the Istituto Neurologico Besta, Milan, Italy), and Monika Rade (Institute of Reconstructive Neurobiology, University of Bonn, Bonn, Germany) for help with in vivo and in vitro experiments; and Elmar Endl for management of flow cytometry (University of Bonn, Bonn, Germany; <http://www.ukb.uni-bonn.de/IMMEI/flowcore/index.html>).

References

- Albini, A., Benelli, R., Noonan, D.M., and Brigati, C. (2004) The "chemoinvasion assay": A tool to study tumor and endothelial cell invasion of basement membranes. *Int. J. Dev. Biol.* **48**, 563–571.
- Apte, S.S., Olsen, B.R., and Murphy, G. (1995) The gene structure of tissue inhibitor of metalloproteinases (TIMP)-3 and its inhibitory activities define the distinct TIMP gene family (erratum in *J. Biol. Chem.* [1996] **271**, 2874). *J. Biol. Chem.* **270**, 14313–14318.
- Arato-Ohshima, T., and Sawa, H. (1999) Over-expression of cyclin D1 induces glioma invasion by increasing matrix metalloproteinase activity and cell motility. *Int. J. Cancer* **83**, 387–392.
- Bachman, K.E., Herman, J.G., Corn, P.G., Merlo, A., Costello, J.F., Cavenee, W.K., Baylin, S.B., and Graff, J.R. (1999) Methylation-associated silencing of the tissue inhibitor of metalloproteinase-3 gene suggests a suppressor role in kidney, brain, and other human cancers. *Cancer Res.* **59**, 798–802.
- Baker, A.H., George, S.J., Zaltsman, A.B., Murphy, G., and Newby, A.C. (1999) Inhibition of invasion and induction of apoptotic cell death of cancer cell lines by overexpression of TIMP-3. *Br. J. Cancer* **79**, 1347–1355.
- Besleaga, R., Montesinos-Rongen, M., Perez-Tur, J., Siebert, R., and Deckert, M. (2003) Expression of the *LGI1* gene product in astrocytic gliomas: Downregulation with malignant progression. *Virchows Arch.* **443**, 561–564.
- Bjerkvig, R., Steinsvag, S.K., and Laerum, O.D. (1986) Reaggregation of fetal rat brain cells in a stationary culture system. I: Methodology and cell identification. *In Vitro Cell Dev. Biol.* **22**, 180–192.
- Brodtkorb, E., Nakken, K.O., and Steinlein, O.K. (2003) No evidence for a seriously increased malignancy risk in *LGI1*-caused epilepsy. *Epilepsy Res.* **56**, 205–208.
- Brodtkorb, E., Michler, R.P., Gu, W., and Steinlein, O.K. (2005) Speech-induced aphasic seizures in epilepsy caused by *LGI1* mutation. *Epilepsia* **46**, 963–966.
- Brustle, O., Jones, K.N., Learish, R.D., Karram, K., Choudhary, K., Wiesler, O.D., Duncan, I.D., and McKay, R.D. (1999) Embryonic stem cell-derived glial precursors: A source of myelinating transplants. *Science* **285**, 754–756.
- Cantley, L.C. (2002) The phosphoinositide 3-kinase pathway. *Science* **296**, 1655–1657.
- Carson, S.D., and Pirruccello, S.J. (1998) Tissue factor and cell morphology variations in cell lines subcloned from U87-MG. *Blood Coagul. Fibrinolysis* **9**, 539–547.
- Chernova, O.B., Somerville, R.P., and Cowell, J.K. (1998) A novel gene, *LG11*, from 10q24 is rearranged and downregulated in malignant brain tumors. *Oncogene* **17**, 2873–2881.
- Cloutier, J.F., Sahay, A., Chang, E.C., Tessier-Lavigne, M., Dulac, C., Kolodkin, A.L., and Ginty, D.D. (2004) Differential requirements for semaphorin 3F and Slit-1 in axonal targeting, fasciculation, and segregation of olfactory sensory neuron projections. *J. Neurosci.* **24**, 9087–9096.
- Fertig, E., Lincoln, A., Martinuzzi, A., Mattson, R.H., and Hisama, F.M. (2003) Novel *LGI1* mutation in a family with autosomal dominant partial epilepsy with auditory features. *Neurology* **60**, 1687–1690.
- Glaser, T., Perez-Bouza, A., Klein, K., and Brustle, O. (2005) Generation of purified oligodendrocyte progenitors from embryonic stem cells. *FASEB J.* **19**, 112–114.
- Goldbrunner, R.H., Bouterfa, H., Vince, G.H., Bernstein, J.J., Roosen, K., and Tonn, J.C. (1997) Transfection and dye premarking of human and rat glioma cell lines affects adhesion, migration and proliferation. *Anticancer Res.* **17**, 4467–4471.
- Gu, W., Brodtkorb, E., and Steinlein, O.K. (2002) *LGI1* is mutated in familial temporal lobe epilepsy characterized by aphasic seizures. *Ann. Neurol.* **52**, 364–367.
- Gu, W., Brodtkorb, E., Piepoli, T., Finocchiaro, G., and Steinlein, O.K. (2005) *LGI1*: A gene involved in epileptogenesis and glioma progression? *Neurogenetics* **6**, 59–66.
- Hedera, P., Abou-Khalil, B., Crunk, A.E., Taylor, K.A., Haines, J.L., and Sutcliffe, J.S. (2004) Autosomal dominant lateral temporal epilepsy: Two families with novel mutations in the *LGI1* gene. *Epilepsia* **45**, 218–222.
- Heldin, C.H., Ostman, A., and Ronnstrand, L. (1998) Signal transduction via platelet-derived growth factor receptors. *Biochim. Biophys. Acta* **1378**, F79–F113.
- Kalachikov, S., Evgrafov, O., Ross, B., Winawer, M., Barker-Cummings, C., Martinelli Boneschi, F., Choi, C., Morozov, P., Das, K., Teplitskaya, E.,

- Yu, A., Cayanis, E., Penchaszadeh, G., Kottmann, A.H., Pedley, T.A., Hauser, W.A., Ottman, R., and Gilliam, T.C. (2002) Mutations in *LG1* cause autosomal-dominant partial epilepsy with auditory features. *Nat. Genet.* **30**, 335–341.
- Krex, D., Mohr, B., Hauses, M., Ehninger, G., Schackert, H.K., and Schackert, G. (2001) Identification of uncommon chromosomal aberrations in the neuroglioma cell line H4 by spectral karyotyping. *J. Neurooncol.* **52**, 119–128.
- Krex, D., Hauses, M., Appelt, H., Mohr, B., Ehninger, G., Schackert, H.K., and Schackert, G. (2002) Physical and functional characterization of the human *LG1* gene and its possible role in glioma development. *Acta Neuropathol. (Berl.)* **103**, 255–266.
- Kunapuli, P., Chitta, K.S., and Cowell, J.K. (2003) Suppression of the cell proliferation and invasion phenotypes in glioma cells by the *LG1* gene. *Oncogene* **22**, 3985–3991.
- Kunapuli, P., Kasyapa, C.S., Hawthorn, L., and Cowell, J.K. (2004) *LG1*, a putative tumor metastasis suppressor gene, controls in vitro invasiveness and expression of matrix metalloproteinases in glioma cells through the ERK1/2 pathway. *J. Biol. Chem.* **279**, 23151–23157.
- Lee, M.K., Tuttle, J.B., Rebhun, L.I., Cleveland, D.W., and Frankfurter, A. (1990) The expression and posttranslational modification of a neuron-specific beta-tubulin isotype during chick embryogenesis. *Cell Motil. Cytoskeleton* **17**, 118–132.
- Marillat, V., Sabatier, C., Failli, V., Matsunaga, E., Sotelo, C., Tessier-Lavigne, M., and Chedotal, A. (2004) The slit receptor *Rig-1/Robo3* controls midline crossing by hindbrain precerebellar neurons and axons. *Neuron* **43**, 69–79.
- Merlo, A., Herman, J.G., Mao, L., Lee, D.J., Gabrielson, E., Burger, P.C., Baylin, S.B., and Sidransky, D. (1995) 5' CpG island methylation is associated with transcriptional silencing of the tumour suppressor *p16/CDKN2/MTS1* in human cancers. *Nat. Med.* **1**, 686–692.
- Michelucci, R., Poza, J.J., Sofia, V., de Feo, M.R., Binelli, S., Bisulli, F., Scudellaro, E., Simionati, B., Zimbello, R., D'Orsi, G., Passarelli, D., Avoni, P., Avanzini, G., Tinuper, P., Biondi, R., Valle, G., Mautner, V.F., Stephani, U., Tassinari, C.A., Moschonas, N.K., Siebert, R., Lopez de Munain, A., Perez-Tur, J., and Nobile, C. (2003) Autosomal dominant lateral temporal epilepsy: Clinical spectrum, new epitempin mutations, and genetic heterogeneity in seven European families. *Epilepsia* **44**, 1289–1297.
- Morante-Redolat, J.M., Gorostidi-Pagola, A., Piquer-Sirerol, S., Sáenz, A., Poza, J.J., Galán, J., Gesk, S., Sarafidou, T., Mautner, V.F., Binelli, S., Staub, E., Hinzmann, B., French, L., Prud'homme, J.F., Passarelli, D., Scannapieco, P., Tassinari, C.A., Avanzini, G., Marti-Massó, J.F., Kluwe, L., Deloukas, P., Moschonas, N.K., Michelucci, R., Siebert, R., Nobile, C., Pérez-Tur, J., and Lopez de Munain, A. (2002) Mutations in the *LG1/Epitempin* gene on 10q24 cause autosomal dominant lateral temporal epilepsy. *Hum. Mol. Genet.* **11**, 1119–1128.
- Muller, P.Y., Janovjak, H., Miserez, A.R., and Dobbie, Z. (2002) Processing of gene expression data generated by quantitative real-time RT-PCR (erratum in *Biotechniques* [2002] **33**, 514). *Biotechniques* **32**, 1372–1374, 1376, 1378–1379.
- Nakano, A., Tani, E., Miyazaki, K., Furuyama, J., and Matsumoto, T. (1993) Expressions of matrilysin and stromelysin in human glioma cells. *Biochem. Biophys. Res. Commun.* **192**, 999–1003.
- Nakayama, J., Fu, Y.H., Clark, A.M., Nakahara, S., Hamano, K., Iwasaki, N., Matsui, A., Arinami, T., Ptacek, L.J. (2002) A nonsense mutation of the *MASS1* gene in a family with febrile and afebrile seizures. *Ann. Neurol.* **52**, 654–657.
- Nolte, C., Matyash, M., Pivneva, T., Schipke, C.G., Ohlemeyer, C., Hanisch, U.K., Kirchhoff, F., and Kettenmann, H. (2001) GFAP promoter-controlled EGFP-expressing transgenic mice: A tool to visualize astrocytes and astrogliosis in living brain tissue. *Glia* **33**, 72–86.
- Okabe, S., Forsberg-Nilsson, K., Spiro, A.C., Segal, M., and McKay, R.D. (1996) Development of neuronal precursor cells and functional post-mitotic neurons from embryonic stem cells in vitro. *Mech. Dev.* **59**, 89–102.
- Ortino, B., Inverardi, F., Morante-Oria, J., Fairén, A., and Frassoni, C. (2003) Substrates and routes of migration of early generated neurons in the developing rat thalamus. *Eur. J. Neurosci.* **18**, 323–332.
- Pilkington, G.J., Bjerkvig, R., De Ridder, L., and Kaaijk, P. (1997) In vitro and in vivo models for the study of brain tumour invasion. *Anticancer Res.* **17**, 4107–4109.
- Pizzuti, A., Flex, E., Di Bonaventura, C., Dottorini, T., Egeo, G., Manfredi, M., Dallapiccola, B., and Giallonardo, A.T. (2003) Epilepsy with auditory features: A *LG1* gene mutation suggests a loss-of-function mechanism (erratum in *Ann. Neurol.* **54**, 137). *Ann. Neurol.* **53**, 396–399.
- Polleux, F., and Ghosh, A. (2002) The slice overlay assay: A versatile tool to study the influence of extracellular signals on neuronal development. *Sci. STKE* **2002**, pl9.
- Ponnio, T., and Conneely, O.M. (2004) *nor-1* regulates hippocampal axon guidance, pyramidal cell survival, and seizure susceptibility. *Mol. Cell. Biol.* **24**, 9070–9078.
- Scheel, H., Tomiuk, S., and Hofmann, K. (2002) A common protein interaction domain links two recently identified epilepsy genes. *Hum. Mol. Genet.* **11**, 1757–1762.
- Senechal, K.R., Thaller, C., and Noebels, J. L. (2005) ADPEAF mutations reduce levels of secreted *LG1*, a putative tumor suppressor protein linked to epilepsy. *Hum. Mol. Genet.* **14**, 1613–1620.
- Skradski, S.L., Clark, A.M., Jiang, H., White, H.S., Fu, Y.H., and Ptacek, L.J. (2001) A novel gene causing a Mendelian audiogenic mouse epilepsy. *Neuron* **31**, 537–544.
- Somerville, R.P., Chernova, O., Liu, S., Shoshan, Y., and Cowell, J.K. (2000) Identification of the promoter, genomic structure, and mouse ortholog of *LG1*. *Mamm. Genome* **11**, 622–627.
- Tenan, M., Benedetti, S., and Finocchiaro, G. (1995) Deletion and transfection analysis of the *p15/MTS2* gene in malignant gliomas. *Biochem. Biophys. Res. Commun.* **217**, 195–202.
- Yang, J., Houk, B., Shah, J., Hauser, K.F., Luo, Y., Smith, G., Schauwecker, E., and Barnes, G.N. (2005) Genetic background regulates semaphorin gene expression and epileptogenesis in mouse brain after kainic acid status epilepticus. *Neuroscience* **131**, 853–869.
- Yuan, W., Zhou, L., Chen, J.H., Wu, J.Y., Rao, Y., and Ornitz, D.M. (1999) The mouse *SLIT* family: Secreted ligands for *ROBO* expressed in patterns that suggest a role in morphogenesis and axon guidance. *Dev. Biol.* **212**, 290–306.